Large Aperture X-ray Refractive Lens from Lithium

N. R. Pereira[*], E. M. Dufresne[†,**] and D. A. Arms[†]

[*]*PO Box 528, Springfield, VA 22152, email=pereira@speakeasy.net*
[†]*X-ray Science Division, Argonne National Division, Argonne, IL 60439*
[**]*Formerly at the Department of Physics, The University of Michigan, Ann Arbor MI 48109*

Abstract. Lithium's low X-ray absorption should give refractive X-ray optics their highest possible performance. We made low-cost lithium lenses that are easy to align and match the ~ 1 mm beam size. This paper summarizes lithium lens performance to date, and what might be done in the future.

Keywords: refractive optics
PACS: PACS number(s): 07.85.Qe

INTRODUCTION

Refractive X-ray optics for synchrotrons[1] became an interesting alternative to mirrors and zone plates optics after the first demonstration of the Compound Refractive Lens (CRL)[2]. Compared to those for visible light, X-ray refractive lenses are weak because the index of refraction $n = 1 - \delta + i\beta$ for X-rays differs so little from unity. A recent article[3] summarizes the accomplishments of a most active group in this field. Their lenses are parabolas because these lack spherical aberration, and the lens curvature decouples from the aperture[4]: N lenslets with a radius of curvature R_0 in series have a focus at $f = R_0/2N\delta$.

Without optical equivalent is Cederstrom's multi-prism[5]. The multi-prism cleverly adds the small deflection of X-rays in each prism to approximate a parabolic lens. The path length of the X-rays is linear with the distance to a prism's top, hence summing the linear paths gives a parabola when the prisms span the X-ray beam under an angle. The parabola's effective radius depends on the multi-prism angle to the X-ray beam path, giving the multi-prisms a simple way to change its focal length. And, prisms are easier to make than parabolas.

The performance of a refractive X-ray lens is a function of δ/β, i.e. the ratio of the index of refraction decrement over the absorption coefficient. Because lithium produces the largest phase shifts per unit absorption length of all solids, we[6, 7, 8, 9] and others[10, 11] use lithium in the best available lens designs[4, 5].

Micro-focusing optics have short X-ray path lengths, so that X-ray attenuation is less important in micro-focusing than for a condenser lens whose purpose is the opposite: gathering most of the X-ray beam into a smaller spot that may match a particular experiment or another X-ray optic's aperture. Such a condenser lens has an aperture that is comparable to the incoming beam (about 1 mm for our beam), while the focus should be $\simeq 0.1$ mm or so. A one-dimensional multi-prism that squeezes a rectangular X-ray beam into a square is also useful. Lithium's long X-ray attenuation length ℓ ($\ell \simeq 60$ mm at 10 keV) is ideal for an X-ray condenser.

For lithium X-ray lenses the main issues are fabrication and corrosion. Corrosion is not noticeable: our lithium lens prototypes focus X-rays just as well in 2006 as they did a few years earlier. But, lithium fabrication methods must become better to achieve the theoretical performance predicted for X-ray optics from lithium. Lithium is easy to shape by embossing or molding. However, standard metal dies can cause problems because lithium tends to stick to metals. A good die material for lithium is polypropylene, which can be used even without lubrication provided that the sliding angle between die and lithium is limited. For the parabola our limit is $60°$, which gives a 1 mm aperture lens a radius of curvature $R_0 \simeq 0.263$ mm. For the multi-prism a convenient die is a polycarbonate Fresnel beam splitter that comes with 0.5 mm high rectangular prisms and a sliding angle of $45°$ angle. The multi-prism needs only a single pressing, while the parabolic lenslets are pressed individually.

The lens packaging in Fig. 1 lets X-rays in and out through 10 mm diameter and 0.126 mm thick beryllium windows in the center of two 70 mm ConFlat flanges connected by a glass tube. The package is high-vacuum quality, but not under vacuum: it contains a slight overpressure of helium. A lithium getter visible through the glass gives additional protection: when the getter remains shiny, the lithium in the lens should be clean too.
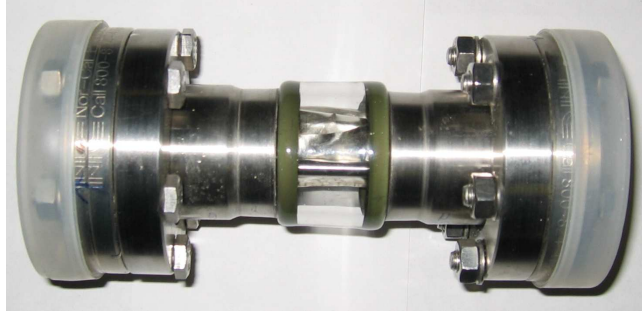
FIGURE 1. Lithium lens packaging.

PARABOLIC CRL FROM LITHIUM

Figure 1 contains a 76-lenslet CRL.[9] The two parabolas in each lenslet are together just under 1 mm thick, but because of the $d \simeq 50$ to 100 μm dead layer between the parabolas and the slight spacing between the lenslets, the total lens is about 100 mm long. The dead layers in a lithium lens absorb a negligible amount of the hard X-rays (at 10 keV about 10%).

Figure 2 is a result from this parabolic lithium lens at 10 keV, and Fig. 3 below has similar data for a two-dimensional multi-prism lens. The measurement setup is straightforward[12]. Briefly, monochromatic[13] X-rays from the Advanced Photon Source's (APS's) beam line 7-ID pass through various beryllium and kapton windows, and a rectangular aperture in front of the lens. A YAG:Ce scintillating screen converts the X-rays into visible light that is observed by a CCD at 5× magnification[14]. The setup is ideal to quickly focus the beam, and adequate to evaluate the quality of the X-ray optic. The CCD is linear, in observation time and in X-ray intensity up to 75 % of the maximum pixel value (4095). In some measurements the X-ray intensity exceeded the linear range, leaving some caveats in the X-ray transmission and gain that must be resolved by independent measurements in the future.

Given that lithium's $\delta \simeq 0.95 \times 10^{-6}$ at 10 keV, the 76-lenslets CRL has a nominal focal length $\simeq 1.82$ m. An X-ray source $d_s = 49.4$ m before the lens then puts the image $d_i = 1.89$ m behind the lens. However, the smallest X-ray spot is found at 1.52 m from the lens, about 0.3 m closer than it should be even when correcting for the lens length (0.1 m).

The left part of Fig. 2 is the unfocused beam apertured to a 500 μm square before the lens, seen by the diagnostics 1.52 m behind the lens as a 515 μm square. Fresnel fringes are visible only along the top and bottom edges because the source penumbra from the slit is much smaller in the vertical than horizontal direction due to the ratio of the source sizes. Thanks to continuous improvements in the beam line, the horizontal striations are smaller here than in previous measurements[8] and Fig. 3.

The right part of Fig. 2 is the best X-ray focus, after attenuation with 0.038 mm aluminum to bring the intensity into the CCD's range. The aluminum reduces the fundamental X-rays at energy $E_1 \simeq 10$ keV about 250-fold, while the beam's harmonics at $E_3 = 3E_1 \simeq 30$ keV decrease by only 0.8 or so and become visible. This is convenient for focusing: a cylindrically symmetric lens has its focus on the beam axis, so that the best orientation of the lens is when the bright focus is in the center of the harmonic beam.

The index of refraction decrement $\delta \propto 1/(E)^2$ for photon energy E, hence he third harmonic deflects $1/9^{th}$ less than the fundamental. In the focal plane for the 10 keV X-rays, the harmonic X-rays at 30 keV give a factor $1 - (1/3)^2$ = 8/9 smaller beam than the original as is indeed seen on the right side of Fig. 2. However, the square is slightly distorted, due to a $\simeq 0.1$ mm misalignment of the individual lenslets[9] that gives the edge of the lens a small deviation from the ideal parabolic profile. Improvements[11] to the molding and mounting hardware are needed to minimize misalignment.

At 10 keV the lens has an X-ray transmission of $T \simeq 0.5$, and a 50-fold intensity gain G that is an order of magnitude lower than the theoretical $G \simeq TM^2 \simeq 500$. The difference is mostly due to the larger image. An ideal image is a demagnified X-ray source, with a demagnification factor $M = d_s/d_i \simeq 32.5$. The source's FWHM is 478 μm horizontal and 33 μm vertical, hence the ideal image is a $\simeq 15$ μm long needle of $\simeq 1$ μm height. The resolution of the diagnostics[14] is $\simeq 5$ μm, and the expected image is therefore 15.5 μm wide by 5 μm high.

Horizontally the FWHM is 36 μm, about 20 μm more than expected. Vertically the FWHM is 26 μm, also 20 μm too large. The focal region is consistent with a demagnified image widened by isotropic scattering over a $\simeq 13$ μradian angle. Some motion of the beam in the vertical direction, as could sometimes be seen with a faster CCD (with lower
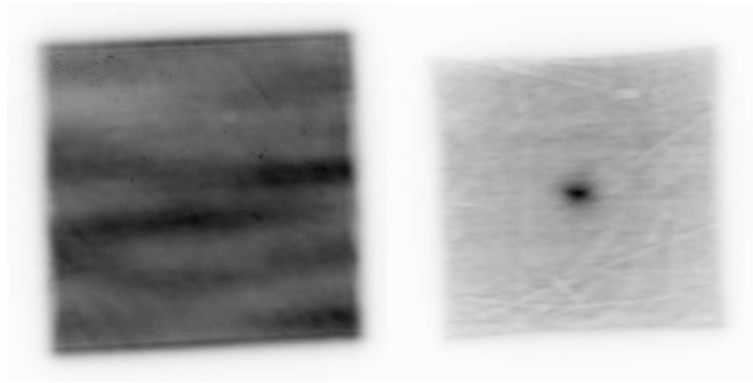
FIGURE 2. Unfocused X-ray beam (left) and focus 1.52 m downstream (behind X-ray filter, right).

dynamic range) may explain some of this broadening. The actual versus theoretical performance of the lenses must be a fabrication issue that we have yet to identify.

Somewhat higher intensities in the focal spot are achieved by opening up the beam-limiting apertures. A 0.7 mm square beam just fits inside the lens' 1 mm diameter, while a 1 mm square beam is not fully captured. The focal spot becomes up to 30 % more intense, but is is also larger and harder to interpret.

TWO DIMENSIONAL FOCUSING WITH MULTI-PRISMS

Fig. 2 for a parabolic lens is similar to Fig. 3, the two-dimensional focus obtained by placing two multi-prisms under $90°$ in a single housing. The left side of Fig. 3 is the 0.5 mm by 0.5 mm square incoming beam, the right side is the image at the focus. In this image the focus is in the upper right corner of the original beam. The X-ray transmission of the two lenses is comparable, but here the gain is $G \simeq 18$. Another difference with Fig. 2 is the spot's asymmetry.

The lithium multi-prism lens has similar problems as discussed for a multi-prism monochromator[15], notably the imperfect shape of the prism's peaks and their counterpart, the valleys. Imperfections along the prism's peaks show up as an irregular focal line, narrower in some places than in others. Mounting two multi-prisms in a single housing allows the two-dimensional lens to align with only a single manipulator, but the fixed position of the multi-prisms with respect to each other rules out optimizing the focus. Cederstrom's original lens doubles the aperture of the lens in Fig. 3, with two opposing multi-prisms in each dimension. The two additional multi-prisms, four in total, should give the lens a $4\times$ larger (1 mm by 1 mm) aperture and up to a fourfold gain, from $G \simeq 18$ to perhaps 72 but more likely lower. The gain from such a multi-prism would be comparable to the 50-fold gain of the parabolic lens, but over a larger spot.

CONCLUSION

Future work should improve lithium manufacture, with as purpose to make lithium X-ray optics approach its theoretical performance. Lithium's corrosion is not a primary issue: the lens in Fig. 3, which was made inside a glove box from extruded strips that lack an oxide layer, behaves little better than an earlier lens that may have had an oxide layer.

Probing the lens locally, with a 20 μm square beam,[9] indicates that the lens is quite good at some locations but does not have the same quality over its entire surface. X-rays scatter everywhere across the lens, but scattering by itself gives no clue to its origin: possible causes are surface imperfections and non-uniformities in the bulk lithium material. Getting distortion and scattering under control is essential for better lenses.

One issue is fundamental: what is the X-ray optical quality of lithium metal after extrusion and molding? Plastic deformation creates dislocations, which may cause X-ray scattering from nominally uniform material. Good lenses use optical-quality glass that is amorphous, uniform, and stress-free, quite unlike the polycrystalline lithium metal that is forced into the shape desired for X-ray lenses.

Research on lithium's metallurgy[16, 17] emphasizes lithium's unique status as a model for bcc metals. Lithium metal is polycrystalline, fully annealed since lithium's melting point ($T_m \simeq 453$ K) is so low that annealing occurs at
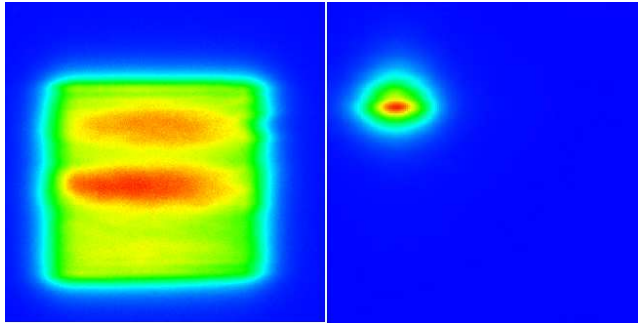
FIGURE 3. Focusing by two multi-prisms under $90°$ with each other in a single housing.

room temperature (at about $2/3 \times T_m$ for bcc metals). It is not obvious that lithium mistreated by extrusion and molding can have the requisite X-ray optics-quality: this can be verified from the X-ray phase behind two nominally uniform cylinders of lithium with different lengths.

Despite the need for further research to make still better X-ray optics from lithium, the $T \simeq 0.5$ X-ray transmission and 50-fold gain already available from lithium lenses is unquestionably useful for many experiments on the beam line. In particular, lithium lenses are much easier to handle than what was feared earlier: proper packaging guarantees that the lithium lenses behave the same now as when they were made a few years ago.

ACKNOWLEDGMENTS

REFERENCES

1. S. Suehiro, H. Miyaji, and H. Hayashi, *Nature* **352**, 385 (1991).
2. A. Snigirev, V. Kohn, A. Snigireva, and B. Lengeler, *Nature* **384**, 49 (1996).
3. B. Lengeler, C. G. Schroer, M. Kuhlmann, B. Benner, T. G. Günzler, O. Kurapova, F. Zontone, A. Snigirev, and I. Snigireva, *J. Phys. D: Appl. Phys.* **38**, A218–A222 (2005).
4. B. Lengeler, C. Schroer, J. Tuemmler, B. Benner, M. Richwin, A. Snigirev, I. Snigireva, and M. Drakopoulos, *J. Synchrotron Rad.* **6**, 1153 (1999).
5. B. Cederstrom, R. Cahn, M. Danielsson, M. Lundqvist, and D. Nygren, *Nature* **404**, 951 (2000).
6. E. M. Dufresne, D. A. Arms, S. B. Dierker, R. Clarke, N. R. Pereira, and D. Foster, *Appl. Phys. Lett.* **79**, 4085 (2001).
7. D. A. Arms, E. M. Dufresne, S. B. Dierker, R. Clarke, N. R. Pereira, and D. Foster, *Rev. Sci. Instrum.* **73**, 1492 (2002).
8. N. R. Pereira, E. M. Dufresne, D. A. Arms, and R. Clarke, *Rev. Sci. Instrum.* **75**, 37 (2004).
9. N. R. Pereira, E. M. Dufresne, D. A. Arms, and R. Clarke, *Proc. SPIE* **5539**, 174–184 (2004).
10. J. T. Cremer, H. R. Beguiristain, M. A. Piestrup, and C. K. Gary, *Rev. Sci. Instrum.* **74**, 2262 (2003).
11. C. Young, *Focusing Optics for X-ray Applications*, Master's thesis, Illinois Institute of Technology (2005).
12. E. M. Dufresne, N. R. Pereira, and D. Arms, *Proc. 2003 SRI Conference and AIP Conference Proceedings* **705** (2004).
13. E. M. Dufresne, D. Arms, S. Dierker, R. Clarke, Y. Yacoby, J. Pitney, B. MacHarrie, , and R. Pindak, *Rev. Sci. Instrum.* **73**, 1511 (2002).
14. E. M. Dufresne, N. R. Pereira, D. Arms, and P. Ilinsky, *Proc. 2003 SRI Conference and AIP Conference Proceedings* **705** (2003).
15. W. Jark, *X-Ray Spectrom.* **33**, 455–461 (2004).
16. M. Krystian, and W. Pichl, *Phys. Rev. B* **62**, 13956 (2000).
17. M. Krystian, and W. Pichl, *Materials Characterization* **46**, 1 (2001).